

ESI† for

A High Dielectric Constant Non-fullerene Acceptor for Efficient Bulk-Heterojunction Organic Solar Cells

Xi Liu,^{‡a} Boming Xie,^{‡a} Chunhui Duan,^{*a} Zhaojing Wang,^a Baobing Fan,^a Kai Zhang,^a Baojun Lin,^b Fallon J. M. Colberts,^c Wei Ma,^{*b} René A. J. Janssen,^c Fei Huang^{*a} and Yong Cao^a

^aState Key Laboratory of Luminescent Materials and Devices, Institute of Polymer Optoelectronic Materials and Devices, South China University of Technology, Guangzhou 510640, P. R. China. *E-mail: duanchunhui@scut.edu.cn; msfhuang@scut.edu.cn

^bState Key Laboratory for Mechanical Behavior of Materials, Xi'an Jiaotong University, Xi'an 710049, P. R. China. *Email: msewma@mail.xjtu.edu.cn

^cMolecular Materials and Nanosystems, Institute for Complex Molecular Systems, Eindhoven University of Technology, P. O. Box 513, 5600 MB Eindhoven, The Netherlands.

‡ These authors contributed equally to this work.

Experimental Section

General Details. All reagents, unless otherwise specified, were obtained from Alfa Aesar or Sigma-Aldrich and used without further purification. Some of the solvents used were further purified before use (THF from sodium/benzophenone, toluene was washed with H₂SO₄ and then treated with CaCl₂). ¹H and ¹³C NMR spectra were measured using a Bruker AV-500. Chemical shifts were expressed in parts per million (ppm), and splitting patterns are designated as s (singlet), d (doublet) and m (multiplet). MS was performed by using a Waters ACQUITY® SQD/TQD for APCI-HRMS and a Waters Vion IMS QToF for MALDI-TOF. UV-vis spectra were recorded on a HP 8453 spectrophotometer. Cyclic voltammetry data were measured on a CHI600D electrochemical workstation by using Bu₄NPF₆ (0.1 M) in acetonitrile as electrolyte and glassy-carbon, platinum, and saturated calomel electrode as the working, counter, and

reference electrode, respectively. Potentials were referenced to the ferrocenium/ferrocene couple by using ferrocene as an internal standard.

Fabrication and characterization of solar cells. The ITO glass substrates were cleaned sequentially under sonication with acetone, detergent, deionized water, and isopropyl alcohol and then dried at 70 °C in a baking oven overnight, followed by a 4-min oxygen plasma treatment. The single component homojunction architecture was ITO/PEDOT:PSS/ITIC-OE or ITIC/Ca/Al. The ~80 nm ITIC-OE or ITIC film was formed by spin-coating the single component solution on top of the PEDOT:PSS layer. After that, an 8 nm Ca layer and a 100 nm Al layer were sequentially deposited by thermal evaporation through a shadow mask in a vacuum chamber at a pressure of 5×10^{-7} torr. The BHJ OSCs with a conventional device structure of ITO/PEDOT:PSS/BHJ active layer/PFN-Br/Ag were fabricated. First, PEDOT:PSS (CLEVIOS™ P VP AI 4083) was spin-coated on top of a cleaned ITO and annealed in air at 150 °C for 15 min to form ~40 nm layer. Subsequently, the active layer with an optimal thickness of ca. 100 nm was formed by spin-coating the mixed solution of PBDB-T and ITIC-OE or ITIC in chlorobenzene (with 0.5% DIO v/v) on top of the PEDOT:PSS layer. After that, the active layers were annealed at 120 °C for 10 min. After spin-coating of 5 nm PFN-Br as cathode interface, a 100 nm Ag layer were sequentially deposited by thermal evaporation through a shadow mask in a vacuum chamber at a pressure of 4×10^{-7} torr. The active layer area of the device was defined to be 0.0516 cm², which was further confined as 0.04 cm² by anon-refractive mask to improve the accuracy of measurements. The photovoltaic performance was measured under an AM 1.5G solar simulator (Taiwan, Enlitech SS-F5). The current density-

voltage (J - V) characteristics were recorded with a Keithley 2400 source meter. The light intensity was 100 mW cm^{-2} as calibrated by a China general certification center (CGC) certified reference monocrystal silicon cell (Enlitech). The external quantum efficiency (EQE) spectra were performed on a commercial EQE measurement system (Taiwan, Enlitech, QE-R3011). The light intensity at each wavelength was calibrated by a standard single-crystal Si photovoltaic cell.

Fabrication and characterization of SCLC devices. Devices were fabricated to measure hole and electron mobility by using the space-charge-limited current (SCLC) method. The device structures of the hole-only devices and electron-only are ITO/PEDOT:PSS/blend films/MoO₃/Ag and ITO/ZnO/blend films/PFN-Br/Ag, respectively. The mobility was determined by fitting the dark current to the model of a single-carrier SCLC model, which is described by the equation $J = (9/8)\epsilon_0\epsilon_r\mu((V^2)/(d^3))$, where J is the current, μ is the zero-field mobility, ϵ_0 is the permittivity of free space, ϵ_r is the relative permittivity of the material, d is the thickness of the active layers, and V is the effective voltage. The effective voltage was obtained by subtracting the built-in voltage (V_{bi}) and the voltage drop (V_s) from the series resistance of the whole device except for the active layers from the applied voltage (V_{appl}), $V = V_{appl} - V_{bi} - V_s$. The charge carrier mobility can be calculated from the slope of the $J^{1/2} \sim V$ curves.

Transmission electron microscopy (TEM). Transmission electron microscopy was performed on a Tecnai G2 Sphera transmission electron microscope (FEI) operated at 200 kV.

Atomic force microscope (AFM). Tapping-mode AFM images were obtained by using a Bruker Multimode 8 Microscope.

PL quenching experiments. The PL quenching experiments were recorded by Shimadzu RF-6000 spectrometer @ different excitation wavelengths for the corresponding films.

Measurements of dielectric constant. The dielectric constants of the materials were determined by the capacitance–voltage (C – V) measurements with a device structure of ITO/PEDOT:PSS/test film (100 nm)/Ca/Al. First, PEDOT:PSS (CLEVIOS™ P VP AI 4083) was spin-coated on top of a cleaned ITO and annealed in air at 150 °C for 15 min to form ~40 nm layer. Subsequently, the test film with the thickness of ca. 100 nm was formed by spin-coating the mixed solution of PBDB-T, ITIC-OE or ITIC in chlorobenzene on top of the PEDOT:PSS layer. After that, a 10 nm Ca and 100 nm Al layer were sequentially deposited by thermal evaporation through a shadow mask in a vacuum chamber at a pressure of 4×10^{-7} torr. The C – V measurements of the molecules were performed using a HP 4192A LCR meter by sweeping the voltage from –30 V to 10 V at room temperature, with ramping rate of 0.5 V s^{-1} and 30 mV of oscillator levels. The measurements were performed under the frequency from 1×10^3 to 1×10^6 Hz. The relative dielectric constants (ϵ_r) were calculated from the equation of $\epsilon_r = Cd/\epsilon_0 A$, where C is the capacitance, d is the thickness of the tested film, ϵ_0 is the permittivity of free space, A is the device area (0.0516 cm^2).

Contact angle measurements. The contact angle tests were performed on a Dataphysics OCA40 Micro surface contact angle analyzer. The surface energy of the polymers was characterized and calculated by the contact angles of the two probe liquids with the Owens and Wendt equation: $(1 + \cos\theta)\gamma_{pl} = 2(\gamma_s^d\gamma_{pl}^d)^{1/2} + 2(\gamma_s^p\gamma_{pl}^p)^{1/2}$, where γ_s and γ_{pl} are the surface energy of the sample and the probe liquid, respectively. The superscripts d and p refer to the dispersion and polar components of the surface energy, respectively.

GIWAXS experiments. Grazing Incidence Wide-Angle X-ray Scattering (GIWAXS) Characterization: GIWAXS measurements were performed at beamline 7.3.3 at the Advanced Light Source. Samples were prepared on Si substrates using identical blend solutions as those used in devices. The 10 keV X-ray beam was incident at a grazing angle of 0.12°-0.16°, selected to maximize the scattering intensity from the samples. The scattered x-rays were detected using a Dectris Pilatus 2M photon counting detector.

Synthesis.

1-Bromo-4-((2-methoxyethoxy)methyl)benzene (1): 4-Bromobenzyl bromide (24.8 g, 100 mmol) and 2-methoxyethanol (9.12 g, 120 mmol) were dissolved in 100 mL THF under argon. Then NaH (2.4 g, 100 mmol) was added quickly, and the reaction solution was continuously stirred for 12 h at ambient temperature. The resulting mixture was pour into ice water and extracted with CH₂Cl₂, after removing the CH₂Cl₂ solvent, the residue was further purified by silica gel column chromatography (petroleum ether) to afford **1** (20 g, 83%) as a colorless oil. ¹H NMR (500 MHz, CDCl₃) δ 7.49 – 7.44 (m, 2H), 7.25 – 7.19 (m, 2H), 4.52 (s, 2H), 3.63 –

3.54 (m, 4H), 3.39 (s, 3H). ^{13}C NMR (125 MHz, CDCl_3): δ 136.40, 131.01, 129.21, 122.42, 74.35, 71.62, 69.61, 59.74. (APCI-HRMS) calcd for $\text{C}_{10}\text{H}_{13}\text{O}_2\text{Br}$, 245.12 found, $[\text{M}^+]$, 244.23.

Diethyl 2,5-bis(thieno[3,2-b]thiophen-2-yl)terephthalate (2): Thieno[3,2-b]thiophene (1.68 g, 12 mmol) was dissolved in 40 mL THF under argon, then 4.8 mL of *n*-BuLi (2.5 M) was dropwise added into the THF solution at $-78\text{ }^\circ\text{C}$, and the reaction solution was continuously stirred for 2h at $-78\text{ }^\circ\text{C}$ and 1h at $-35\text{ }^\circ\text{C}$. Then ZnCl_2 in THF (17.14 mL, 1M) was dropwise added into the reaction solution at $0\text{ }^\circ\text{C}$, and with another 1.5 h stirring for the solution. Then diethyl 2,5-dibromoterephthalate (1.83 g, 4.84 mmol) and 240 mg $\text{Pd}(\text{PPh}_3)_4$ were added into the reaction solution quickly, and the reaction solution was refluxing for 12 h. After removing the solvent, the residue was further purified by silica gel column chromatography (petroleum ether with 10% ethyl acetate) to afford **2** (1.56 g, 65%) as a yellow solid. ^1H NMR (500 MHz, CDCl_3) δ 7.89 (s, 2H), 7.40 (d, $J = 5.2\text{ Hz}$, 2H), 7.29 (dd, $J = 6.7, 0.6\text{ Hz}$, 4H), 4.25 (q, $J = 7.1\text{ Hz}$, 4H), 1.13 (t, $J = 7.1\text{ Hz}$, 6H). ^{13}C NMR (125 MHz, CDCl_3): δ 167.42, 142.13, 139.90, 139.23, 134.01, 133.81, 132.20, 127.44, 119.56, 119.32, 61.68, 13.75. (APCI-HRMS) calcd for $\text{C}_{24}\text{H}_{18}\text{O}_4\text{S}_4$, 498.01; found, $[\text{M}^+]$, 497.03.

IDTT-OE: Compound **1** (0.98 g, 4 mmol) was dissolved in 10 mL THF under argon, then 1.6 mL *n*-BuLi (2.5 M) was dropwise added into the THF solution at $-78\text{ }^\circ\text{C}$, and the reaction solution was continuously stirred for 1h at $-78\text{ }^\circ\text{C}$. Then the compound **2** was dissolved in THF (400 mg of compound **2** in 15 mL THF) dropwise added into the reaction solution, and the reaction solution was warmed to room temperature for another 1h stir. The resulting mixture was pour into ice water and extracted with ethyl acetate, after removing the ethyl acetate, the

residue was dissolved into 50 mL acetic acid with drops of H₂SO₄ for 2 h refluxing. The final resulting mixture was poured into ice water and extracted with ethyl acetate, after removing the ethyl acetate, the residue was further purified by silica gel column chromatography (petroleum ether with 20% ethyl acetate) to afford IDTT-OE (289.8 mg, 35%) as a yellow solid. ¹H NMR (500 MHz, CDCl₃) δ 7.46 (s, 2H), 7.27 (dd, *J* = 8.6, 3.6 Hz, 20H), 4.52 (s, 8H), 3.62 (dd, *J* = 4.0, 1.6 Hz, 8H), 3.56 (dd, *J* = 4.0, 1.6 Hz, 8H), 3.37 (s, 12H). ¹³C NMR (125 MHz, CDCl₃) δ 145.72, 141.32, 140.03, 137.62, 137.21, 136.93, 136.85, 136.80, 135.20, 134.54, 128.66, 128.15, 124.82, 123.81, 120.75, 119.55, 71.98, 70.93, 69.69, 62.14, 59.12. MS (MALDI-TOF) calcd for C₆₀H₅₈O₈S₄, 1035.36; found [M], 1035.47.

IDTT-OE-CHO: IDTT-OE (200 g, 0.19 mmol) was dissolved in 20 mL dichloroethane under argon, then the fresh POCl₃ solution (0.24 mL POCl₃ in 3.5 mL DMF) was dropwise added into the mixture at 0 °C, and the reaction solution was continuously stirred for 24 h at 60 °C. After removing the solvent, the residue was further purified by silica gel column chromatography (dichloromethane with 20% ethyl acetate) to afford **IDTT-OE-CHO** (147 mg, 70%) as a yellow solid. ¹H NMR (500 MHz, CDCl₃) δ 9.87 (s, 2H), 7.94 (s, 2H), 7.49 (s, 2H), 7.33 – 7.18 (m, 16H), 4.53 (d, *J* = 2.0 Hz, 8H), 3.62 (dd, *J* = 5.1, 3.9 Hz, 8H), 3.56 (dd, *J* = 5.9, 3.1 Hz, 8H), 3.37 (s, 12H). ¹³C NMR (125 MHz, CDCl₃) δ 185.10, 146.52, 142.32, 140.83, 137.92, 137.03, 136.45, 135.83, 135.31, 134.59, 129.26, 128.15, 124.82, 123.81, 120.78, 119.75, 72.08, 71.36, 69.89, 62.65, 59.75. MS (MALDI-TOF) calcd for C₆₂H₅₈O₁₀S₄, 1091.38; found [M + Na], 1114.04.

ITIC-OE: IDTT-OE-CHO (120 mg, 0.11 mmol) and 3-(dicyanomethylidene)indan-1-one (100 mg, 0.51 mmol) were dissolved in 25 mL chloroform under argon, then 1 mL pyridine was added into the solution, and the reaction solution was continuously stirred for 12 h at 50 °C. After removing the solvent, the residue was further purified by silica gel column chromatography (petroleum ether/ethyl acetate) and by GPC HPLC to afford ITIC-OE (119 mg, 75%) as a dark blue solid. ¹H NMR (500 MHz, CDCl₃) δ 8.86 (s, 2H), 8.70 – 8.67 (m, 2H), 8.21 (s, 2H), 7.93 – 7.90 (m, 2H), 7.76 (ddd, *J* = 8.2, 7.2, 3.4 Hz, 4H), 7.59 (s, 2H), 7.36 – 7.26 (m, 16H), 4.54 (s, 8H), 3.67 – 3.60 (m, 8H), 3.59 – 3.52 (m, 8H), 3.36 (s, 12H). ¹³C NMR (125 MHz, CDCl₃) δ 188.10, 160.31, 155.29, 152.65, 147.13, 146.62, 143.65, 140.92, 140.03, 139.62, 138.16, 137.91, 136.93, 136.85, 136.80, 135.21, 134.52, 128.36, 128.05, 125.32, 123.81, 122.94, 118.55, 114.57, 114.51, 72.92, 71.97, 69.69, 69.57, 63.34, 59.09. MS (MALDI-TOF) calcd for C₈₆H₆₆N₄O₁₀S₄, 1442.37; found [M + Na], 1465.05.

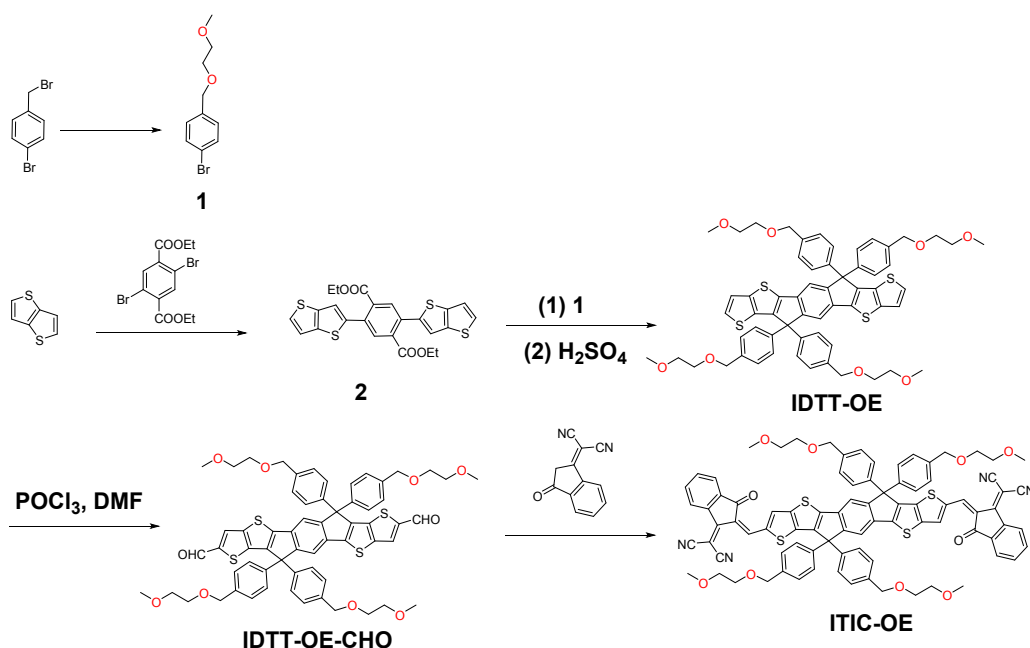


Fig. S1 The synthetic route of ITIC-OE.

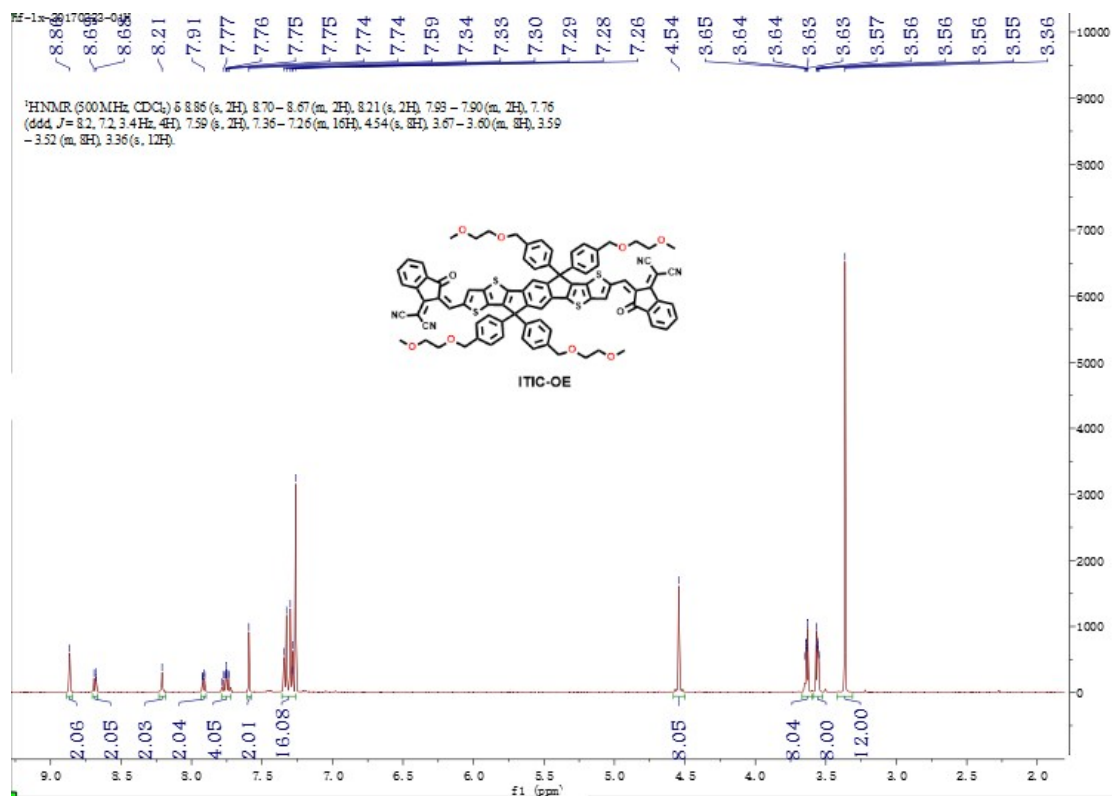


Fig. S2 ¹H NMR spectrum of ITIC-OE solution in CDCl₃.

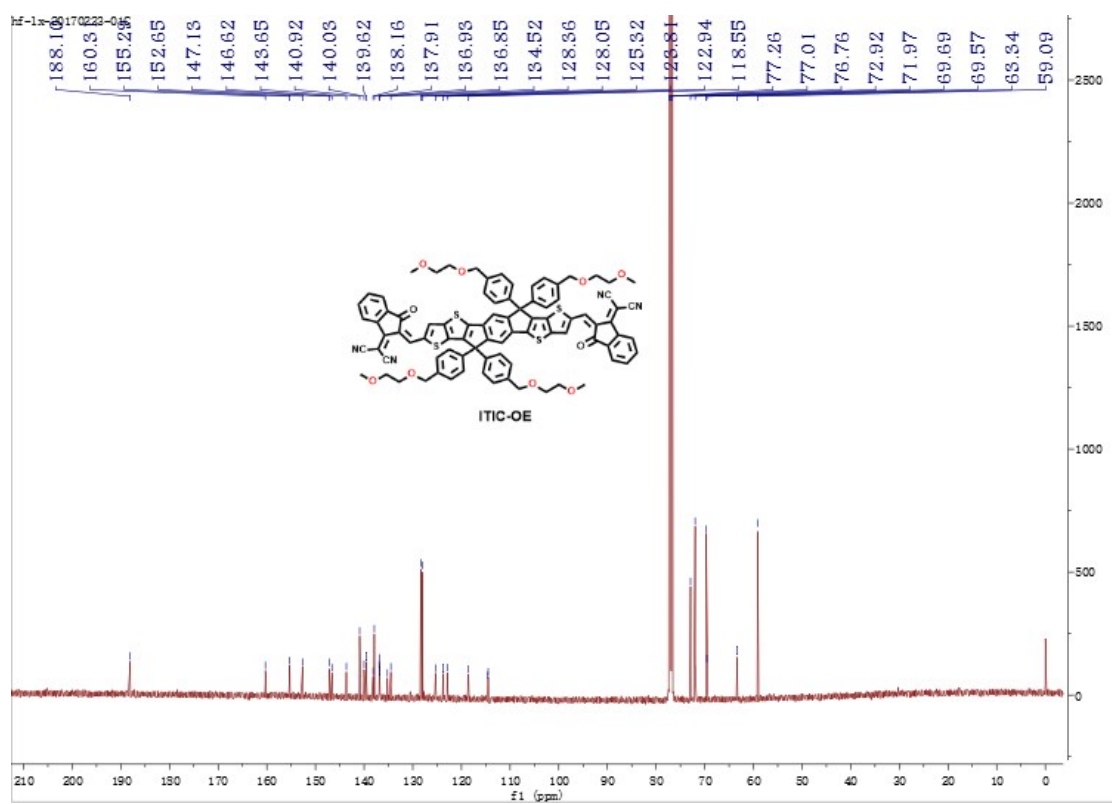


Fig. S3 ¹³C NMR spectrum of ITIC-OE solution in CDCl₃.

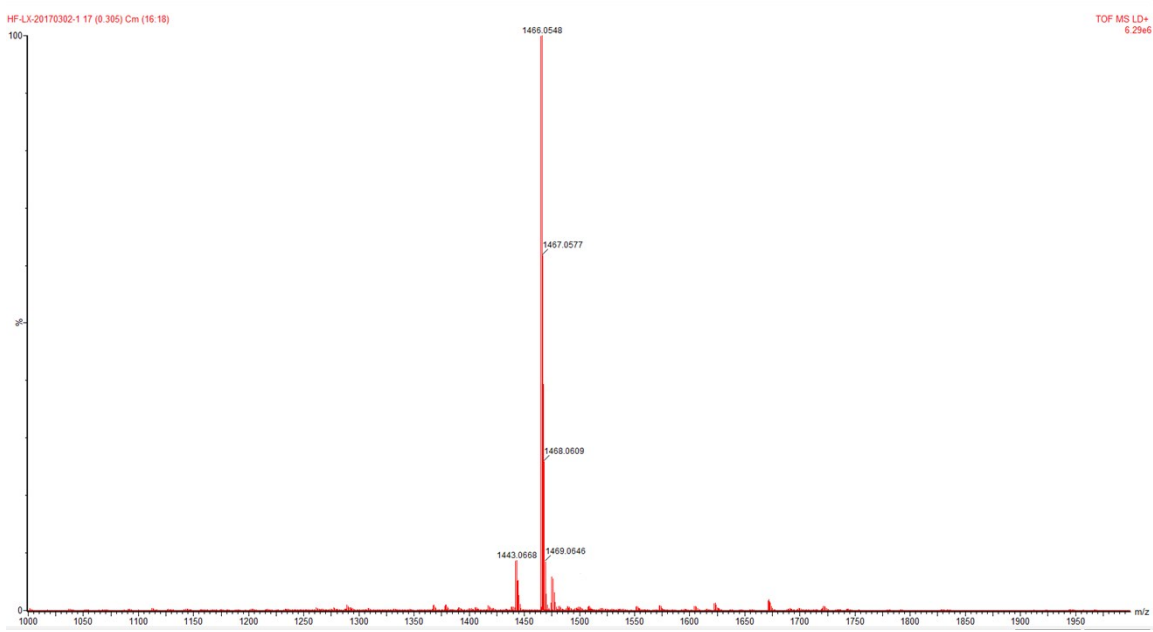


Fig. S4 MS (MALDI-TOF) spectrum of ITIC-OE.

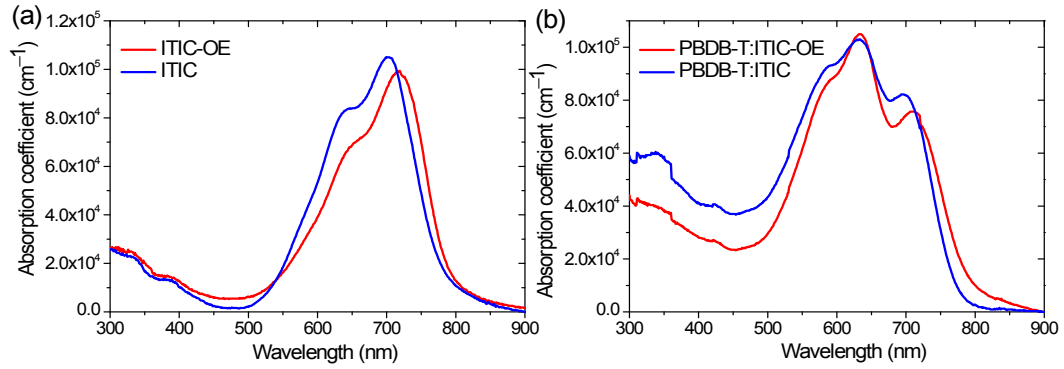


Fig. S5 The absorption coefficient of the ITIC-OE and ITIC pure films (a) and the two corresponding blend films (b).

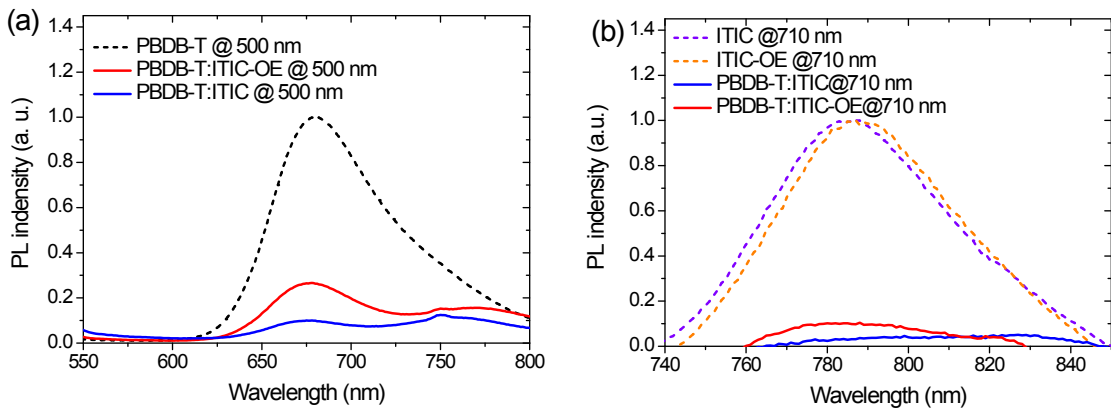


Fig. S6 PL spectra of the PBDB-T pure film and two corresponding blend films excited at 500 nm (a), the ITIC, ITIC-OE pure films and two corresponding blend films excited at 710 nm (b).

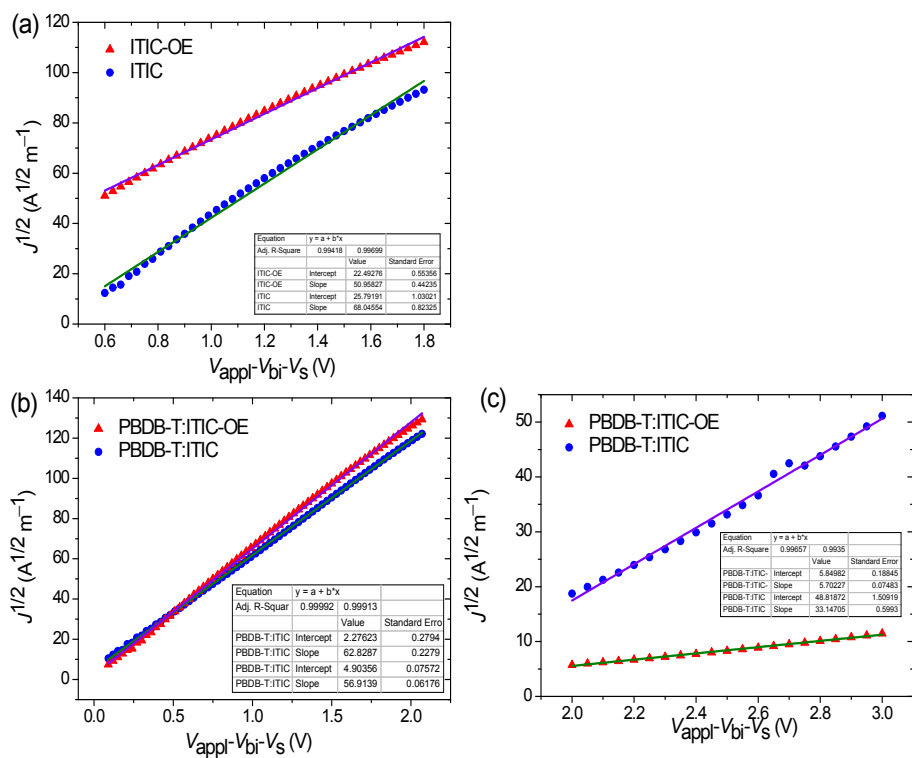


Fig. S7 The $J^{1/2}$ versus $V_{app} - V_{bi} - V_s$ characteristic in SCLC regions of electron-only devices for the ITIC-OE and ITIC pure films (a); hole-only devices (b) and electron-only devices (c) for the corresponding blend films.

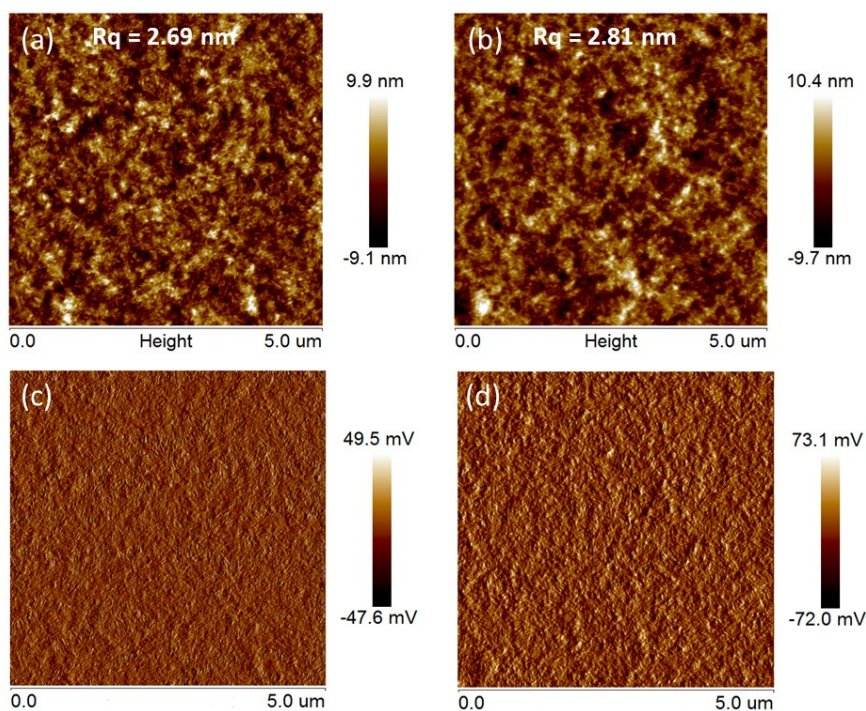
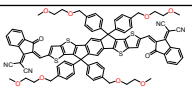
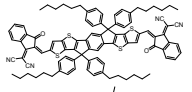
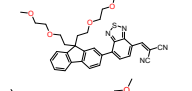
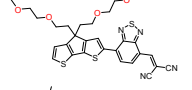
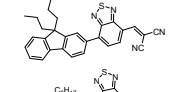
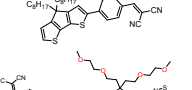
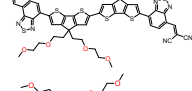
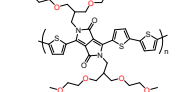
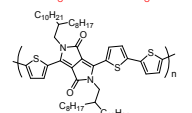


Fig. S8 The AFM topography and phase images of PBDB-T:ITIC-OE blend film (a, c) and PBDB-T:ITIC blend film (b, d).

Table S1 Chemical structures and dielectric constant of the selected organic semiconductors.

Materials	Chemical structures	Dielectric constant ϵ_r	Test frequency (Hz)	Ref.
ITIC-OE		9.4	1.0×10^3	This work
ITIC		4.5	1.0×10^3	This work
M1		8.5	0.8×10^2	[1]
M2		9.8	0.8×10^2	[1]
K12		3.8	0.8×10^2	[1]
M3		4.3	0.8×10^2	[1]
DG		6.1	0.8×10^2	[2]
PDPP3T-O14		5.5	1.0×10^3	[3]
PDPP3T-C20		2.0	1.0×10^3	[3]

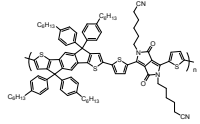
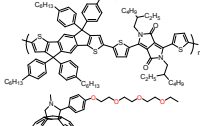
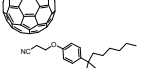


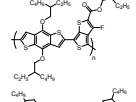
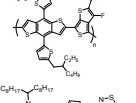
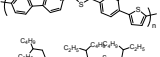
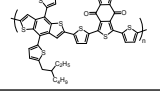
PIDT-DPP-CN		5.0	1.0×10^3	[4]
PIDT-DPP-Alkyl		3.5	1.0×10^3	[4]
PTEG-1		5.7	1.0×10^2	[5]
FCN-n		5.0	1.0×10^3	[6]
PC ₆₁ BM		3.9	1.0×10^3	[5, 6]
PTB7		3.3	1.0×10^3	[7]
PTB7-Th		2.7	1.0×10^3	[7]
PCDTBT		3.2	1.0×10^3	[7]
PBDB-T		2.8	1.0×10^3	This work

Table S2 Photovoltaic properties of OSCs based on PBDB-T:ITIC-OE AM 1.5 G at 100 mW cm⁻². The average values and standard deviation of device statistics from 10 devices.

D:A ratio	Annealing	Thickness (nm)	V_{oc} (V)	J_{sc} (mA cm ⁻²)	FF	PCE (%)	PCE _{max} (%)
1:0.7	120 °C, 10 min	105	0.85 ± 0.01	14.5 ± 0.3	0.65 ± 0.01	8.0 ± 0.1	8.0
1:1	120 °C, 10 min	105	0.85 ± 0.01	14.7 ± 0.1	0.66 ± 0.01	8.2 ± 0.2	8.3
1:1.3	120 °C, 10 min	102	0.85 ± 0.01	13.2 ± 0.1	0.57 ± 0.02	6.4 ± 0.1	6.5
1:1	120 °C, 10 min	70	0.85 ± 0.01	14.4 ± 0.1	0.65 ± 0.01	7.8 ± 0.1	7.9
1:1	120 °C, 10 min	103	0.85 ± 0.01	14.4 ± 0.4	0.69 ± 0.01	8.3 ± 0.1	8.4
1:1	120 °C, 10 min	160	0.85 ± 0.01	14.7 ± 0.1	0.65 ± 0.02	8.2 ± 0.1	8.2
1:1	120 °C, 5 min	100	0.84 ± 0.01	14.8 ± 0.0	0.66 ± 0.01	8.2 ± 0.1	8.3
1:1	120 °C, 10 min	100	0.85 ± 0.01	14.8 ± 0.2	0.67 ± 0.02	8.4 ± 0.3	8.5
1:1	120 °C, 15 min	100	0.85 ± 0.01	14.6 ± 0.1	0.62 ± 0.01	7.7 ± 0.1	7.7
1:1	140 °C, 5 min	105	0.84 ± 0.01	14.8 ± 0.1	0.65 ± 0.02	8.1 ± 0.1	8.2
1:1	140 °C, 10 min	105	0.84 ± 0.01	14.9 ± 0.1	0.62 ± 0.01	8.3 ± 0.1	8.3
1:1	140 °C, 15 min	105	0.84 ± 0.01	14.8 ± 0.2	0.66 ± 0.01	8.2 ± 0.1	8.3
1:1 ^{a)}	120 °C, 10 min	100	0.82 ± 0.00	14.9 ± 0.1	0.67 ± 0.07	8.2 ± 0.1	8.3
1:1 ^{a)}	120 °C, 10 min	100	0.86 ± 0.01	16.2 ± 0.2	0.67 ± 0.08	9.3 ± 0.1 ^{b)}	9.4 ^{b)}

^{a)}Under the invert devices with the structure of ITO/ZnO (40 nm)/BHJ active layer (100 nm)/MoO_x (10 nm)/Ag (100 nm), ^{b)}the data of PBDB-T:ITIC blend films.

Table S3 Summary of the photovoltaic properties based on high dielectric constant organic semiconductors.

Name	Dielectric constant ϵ_r	PCE (%)	V_{oc} (V)	J_{sc} (mA cm ⁻²)	FF	Ref.
ITIC-OE ^{a)}	9.4	8.5	0.85	14.8	0.67	This work

PDPP3T-O14 ^{a)}	5.5	4.5	0.50	16.4	0.55	[4]
FCN-n ^{a)}	5.0	5.6	0.90	8.7	0.71	[6]
PIDT-DPP-CN ^{b)}	5.0	1.4	0.71	3.0	0.68	[3]
M1 ^{c)}	8.5	0.1	0.52	0.81	0.25	[1]
M2 ^{c)}	9.8	0.1	0.40	0.86	0.35	[1]
DG ^{c)}	6.1	0.3	--	--	--	[2]
ITIC-OE ^{c)}	9.4	0.2	0.88	0.80	0.33	This work

^{a)}Bulk heterojunction architecture, ^{b)}bilayer heterojunction architecture, ^{c)}single component homojunction architecture.

Table S4 Hole and electron mobilities obtained by SCLC method.

Active layer	μ_h (cm ² V ⁻¹ s ⁻¹)	μ_e (cm ² V ⁻¹ s ⁻¹)	μ_h/μ_e
ITIC-OE	–	4.8×10^{-4}	–
ITIC	–	6.4×10^{-4}	–
PBDB-T:ITIC-OE	3.5×10^{-4}	1.2×10^{-5}	28.9
PBDB-T:ITIC	3.2×10^{-4}	3.1×10^{-4}	1.0

References

- [1] J. E. Donaghey, A. Armin, P. L. Burn and P. Meredith, *Chem. Commun.*, 2015, **51**, 14115.
- [2] A. Armin, D. M. Stoltzfus, J. E. Donaghey, A. J. Clulow, R. C. R. Nagiri, P. L. Burn, I. R. Gentle and P. Meredith, *J. Mater. Chem. C*, 2017, **5**, 3736.
- [3] N. Cho, C. W. Schlenker, K. M. Kesting, P. Koelsch, H.-L. Yip, D. S. Ginger and A. K. Y. Jen, *Adv. Energy Mater.*, 2014, **4**, 1301857.
- [4] X. Chen, Z. Zhang, Z. Ding, J. Liu and L. Wang, *Angew. Chem. Int. Ed.*, 2016, **55**, 10376.
- [5] F. Jahani, S. Torabi, R. C. Chiechi, L. J. A. Koster and J. C. Hummelen, *Chem. Commun.*, 2014, **50**, 10645.
- [6] S. Zhang, Z. Zhang, J. Liu and L. Wang, *Adv. Funct. Mater.*, 2016, **26**, 6107.